DOI: 10.61782/fa.2023.0448

forum acusticum 2023

PERFORATION RATIO EVALUATION OF LINER TREATMENTS BY EXPERIMENTAL APPROACHES WITH ACOUSTICAL AND OPTICAL METHODS

Jérémie Derré[1*] **Marcelle Gomes**[1] **Nathan Sauron**[2] **Thibault Abily**[2]
[1] Acoustic testing team, Flight test and integration center, Airbus Operations SAS
316 route de Bayonne, 31060 Toulouse Cedex 03, France
[2] Expleo France, 13 rue Marie-Louise Dissard, 31300 Toulouse, France

ABSTRACT

The proposed study compares the perforation ratio estimation of aeronautic liner treatments by acoustic experimental approach, with an image post-processing evaluation method. This need is directly linked to the importance of the perforated sheet lying on the upper part of the treatment, which coupled with the backwards cavities, composes the liner, whose goal is to attenuate the aircraft engine noise. Aside from being the entry door of the treatment, the resistive sheet is the part directly subjected to the aerodynamic flow, leading to efficiency loss due to the drag. Therefore, the perforation of this plate is of paramount importance, and its ratio to the global sheet area plays an important role in it, combined with the perforation shapes and surface roughness. Indeed, the manufacturing tolerances and material defects might impact the resulting percentage of open area, and thus it has to be evaluated directly on the final product. The study presents two approaches with their advantages, limitations and biases: an acoustical evaluation with the Guess model based on experimental impedance testbench data, and a high-resolution image processing based on holes identification by Hough transform and counting.

Keywords: *Acoustics, Optics, Materials, Experimental*

**Corresponding author*: *jeremie.derre@airbus.com.*

1. INTRODUCTION

An acoustic treatment is an assembly of a perforated upper layer (often called resistive layer) opening to one or several cavities, and closed on the other side with a rigid backing skin. In the aerospace industry, and especially in the case of the nacelle of an aircraft engine, the acoustic treatments are called liners, and aim at attenuating the engine noise. These materials are mostly composed of cavities shaped as honeycomb cells of the same size. Such multi-layer materials are usually called SDOF for Single Degree Of Freedom, and work as a combination of 1/4 wavelength and Helmholtz resonators. This treatment design is complex as being a compromise in optimization for multi-physical aspects, like the aerodynamic drag, the added mass or the structural behavior, as well as being optimized for various operational conditions, such as take-off, cruise or approach. As several of these phases are being used for external noise certification with required procedures [1, 2], it is of prime interest to design the most appropriate liners.

One of the upper layer features is its percentage of open area (abbreviated POA, often identified as σ in the acoustic liner literature, and sometimes called perforation ratio). It can be defined as the percentage of the perforation (opening) of a surface compared to the total area of interest. This parameter represents in a way the entrance for the acoustic incident wave to the resonator, and has a large impact on the global acoustic absorption. Generally, the resistive sheet geometric values are given by the suppliers, and are based on the drilling expectations. However, the final effective POA of the liner could differ, because the perforation has bias, such as non perfectly shaped holes,

tolerances or wear of the drilling bits. Moreover, the sheet has to be integrated with the other parts of the liner, and these stages of manufacturing and integration could partially block some holes, by resin migration for instance. So that, the POA experimental evaluation of the complete liner treatment is essential.

In this study, two experimental approaches are proposed for the POA evaluation of aircraft liner samples.

The paper as proposed by the authors is organized in three main parts. The first one introduces some elements of the liner fundamentals as well as the study methodology. The two experimental methods proposed for the POA evaluation of liner samples are described : the acoustical one is based on the measurement of the acoustical response of the liner with an impedance testrig, and the computation of the POA on the resistance function of the excitation acoustic velocity. The second method is based on Hough transform post-processing of a high-resolution image of the same liner sample, to identify the holes and their diameters. Additionally, the in-house impedance bench used for the acoustic measurements, called NTMM, is presented.

The second part details the obtained results. It includes the presentation of the typical impedance measurement, as well as the computation of the acoustical POA on the resistance function of the excitation acoustic velocity. For the optical POA, the complete hole diameters identification is presented and compared.

The third part presents the analysis of the results. The discussion integrates the evaluation of the initial hypothesis limitations, the advantages and drawbacks of each approach, as well as their opportunities. Finally, the methodology and POA results are summarized, as well as the global outcomes of this paper, with the next steps for the continuity of this study.

2. METHODOLOGY AND CHOSEN SPECIMEN

When in a preliminary project for instance, or in the case of complex architectured material, it could sometimes be more straightforward to evaluate experimentally a 3D printed liner concept rather than to run a hundred thousand points FEM computation. Therefore, the POA of the final liner sample to test has to be estimated, integrating all the potential imprecisions of the different stages of the manufacturing and integration.

In addition to the treatment potential defects, any POA evaluation method itself would contain bias. At the Airbus acoustic lab, the classical way to estimate the POA is an acoustical method, based on the experimental measurement of the liner impedance, and explained into details in section 2.2. However, one of these biases, is that as the impedance depends on the level and types of excitation, the sample acoustic answer is intrinsically depending on the procedure and bench used to characterize it. Some effects have already been studied in the literature, such as the influence of the excitation signal (broadband noises, pure or multi sines, sweep sine, or even combination of both), or the impact of its bandwidth, combined with the excitation levels. Previous internal works have explored some of the above-mentioned aspects. However, no general conclusions could be drawn, as strongly depending on the nature of the liner itself.

Meanwhile, it has been decided to perform the work presented in this paper on a given liner, to go further on the acoustical POA evaluation as well as testing another approach, based on an optical method. This liner is somehow representing a SDOF acoustic treatment that could be found in an aircraft jet engine. The resistive sheet of the sample is made of holes that are designed to be cylindrical. The hole diameter D_h is supposed to be the same for every hole of the perforated sheet, the latest assumed to be of constant thickness e_p.

Fig. 1 presents an example of the studied sample (namely Conf 3) of dimensions 400 mm long per 100mm width, with three areas identified for the acoustic measurements, as well as for the optic area of interest.

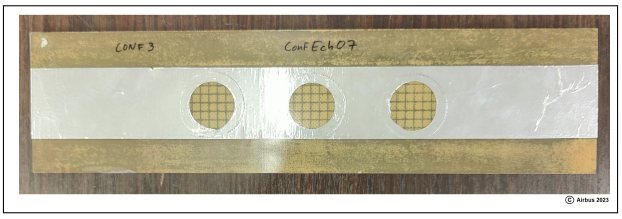

Figure 1. Example of acoustic SDOF liner sample (Conf 3), covered with aluminium tape to identify the areas of interest.

2.1 Liner modelling

In terms of modelling, the liner behaviour is generally represented with a mathematical value called impedance and noted Z. This impedance could be defined as the ratio between the incident pressure over the acoustic flow,

namely the acoustic impedance Z_{ac}, or over the acoustic velocity and thus called the specific acoustic impedance Z_s. These quantities are spatially dependent, due to the geometry and the propagation, but could be homogenised for a material by considering the porosity of the resistive sheet (POA or σ). The real part of the impedance is called the resistance R, and is generally driven by the resistive sheet, whereas the imaginary part called the reactance χ to the cavity, as presented in Eqn. (1)

$$Z_{ac}(\omega) = R(\omega) + j\,\chi(\omega)\,, \tag{1}$$

where the frequency dependence is mentioned with the pulsation ω. It has been shown by some studies that at a certain incident sound pressure level, the resistive sheet also has an impact on the reactance, due among other things to the radiation and visco-thermal losses effects [3].

A classical approach used for the modelling of the perforated plate impedance is the theory of Guess [4]. As aforementioned, the focus is made on the resistive part, which is mainly carried by the perforated plate. The perforated plate impedance Z_G is established following several physical phenomena. The visco-thermal losses are the losses into the boundary layer when passing through the sheet thickness, and are taken into account with the approach of Stinson [5]. The radiation of each hole involves a virtual sheet thickness increase, and so is the resistive response. Moreover, the Guess model assumes that the viscous edges effect strongly depends on the frequency such as the dimension of the system. In order to consider theses conditions, the shear number S_h defined in Eqn. (2) is used to differentiate the low and high frequency regimes

$$S_h = D_h\sqrt{\frac{\omega\rho}{4\mu}}\,, \tag{2}$$

with ρ being the air density and μ the air dynamic viscosity. Thus, it leads to Eqn. (3) for the low frequency impedance Z_G^{LF}, where S_h is smaller than 0.71 so that

$$Z_G^{LF} = \frac{24\,\nu\,(e_p + D_h)}{\sigma\,c\,D_h^2} + j\frac{4\,\omega\,e_p}{3\,\sigma\,c}\,, \tag{3}$$

with ν the kinematic viscosity, and c the wave celerity. For S_h larger than 7.07, the high frequency impedance Z_G^{HF} is defined such as in Eqn. (4)

$$\begin{aligned} Z_G^{HF} &= \frac{2(e_p + D_h)\sqrt{2\,\nu\,\omega}}{\sigma\,c\,D_h} + \dots \\ &\quad j\left(\frac{\omega\,e_p}{\sigma\,c} + \frac{2(e_p + D_h)\sqrt{2\,\nu\,\omega}}{\sigma\,c\,D_h}\right)\,. \end{aligned} \tag{4}$$

The previous formulations do not yet take into account the radiation effect from each hole, as well as their interactions. Nevertheless, in order to simplify the notation and also because only the resistance is studied, the backended cavity and the interaction between holes are not explicited but included into the term δ. When only considering the perforated sheet resistance, the impedance Z_G can be rewritten as Eqn. (5)

$$Z_G = Z_G^{LF/HF} + \left(\frac{D_h\pi^2}{\omega\,c}\sqrt{\frac{2}{\sigma}}\right) + \delta\,. \tag{5}$$

2.2 Acoustical POA evaluation

The results of the acoustical POA are obtained with an in-house impedance tube based on the two microphones method TMM [6, 7]. It follows the usual standards [8, 9] on such testbench as could be found in many acoustic laboratories [10]. This cylindrical waveguide, named NTMM, has a diameter of 30mm and works in the plane waves range [400; 6000] Hz, and at levels between 110 and 160dB. Two 1/4 inch pressure-field microphones are flush mounted. The dispersion and dissipation are considered, the latest being mainly driven by the wall visco-thermal losses modeled as in [11]. A flush mounted sensor measures the fluid temperature in the duct, and is taken into account for the post-processing. Fig. 2 presents an overview of the test rig.

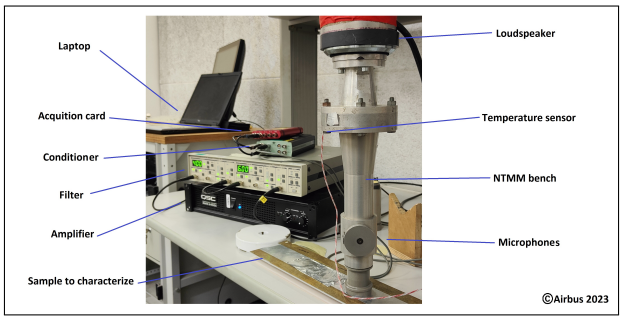

Figure 2. NTMM bench with its full acquisition and generation chains, mounted over a sample.

σ_{ac} the acoustical POA is estimated in the Airbus method by using the non-linear effects [3,12]. The indicator of linear or non-linear behaviour from the system is the Strouhal number S_t, defined in Eqn. (6)

$$S_t = \frac{\omega\,D_h}{2\pi|v|}\,, \tag{6}$$

with v the acoustic velocity. When S_t is smaller than 1 [13], the particle displacement is much larger than the hole diameter and the non-linear regime is assumed. This involves a vortex shedding near the hole apertures, which increases the resistance and generally decreases the reactance due to a lack of radiation. Indeed, the virtual prolongation of the hole corresponding to the acoustic radiation is disturbed and reduced due to the vortex shedding phenomena, which caused the eigenfrequencies shift higher. The evolution of the non-linearity is assumed linear with the acoustic pressure or velocity [12], leading to the formulation of the non-linear part of the resistance $\mathrm{R}(Z_G)_{NL}$ such as Eqn. (7)

$$R(Z_G)_{NL} = R(Z_G) + \frac{(1-\sigma_{ac}^2)|v|}{c\,\sigma_{ac}}\,. \tag{7}$$

σ_{ac} can then be calculated from the measured acoustic impedance in Eqn. (8)

$$\sigma_{ac} = \sqrt{\frac{1}{1+a_{NL}}}\,, \tag{8}$$

where a_{NL} is the slope of the non-linearity evolution of the acoustic resistance function of the acoustic velocity v, since it is considered linear.

2.3 Optical POA evaluation

As already aforementioned, the liner chosen for this study is assumed to have cylindrical holes. Considering this assumption, only the external surface of the sample is taken into account. As a first approach, it is proposed to perform high quality pictures of the samples. For this study, the resolution is 4879 pixels by 5390 pixels. Then, a Circle Hough Transform (CHT) is performed [14]. Such a method is based on a feature identification of a digital image. Many open source codes can be found on the Internet, with several levels of input parameters and complexity. In this paper, an *a priori* knowledge of the resistive sheet is available : the hole distribution pattern is assumed to be known and constant (so that the distance inter-holes), and the drilling diameter also (or at least comprise in a small interval around the target value of 0.5mm).

3. RESULTS

This part presents the results for the two approaches studied in this paper.

Fig. 3 illustrates the normalized acoustic resistance function of the frequency of the Conf 3 sample excited at 130dB with the NTMM bench, for the three positions of Fig. 1, with additional repeatability and reproducibility measurements performed. The purple area represents the frequency interval of integration of the resistance, which is averaged and plotted in Fig. 4 as function of the associated acoustic velocity of all the excitation signals.

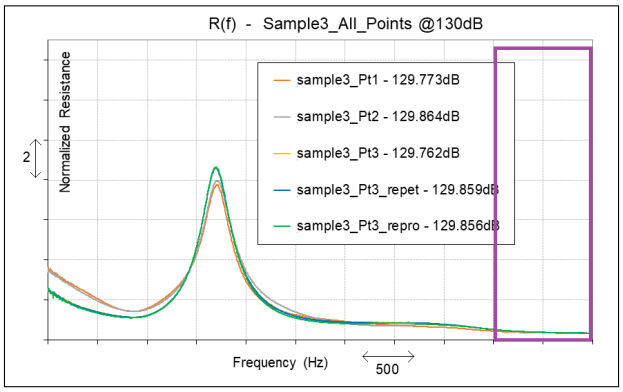

Figure 3. Normalized acoustic resistance function of the frequency for several measurements performed on the Conf 3 sample.

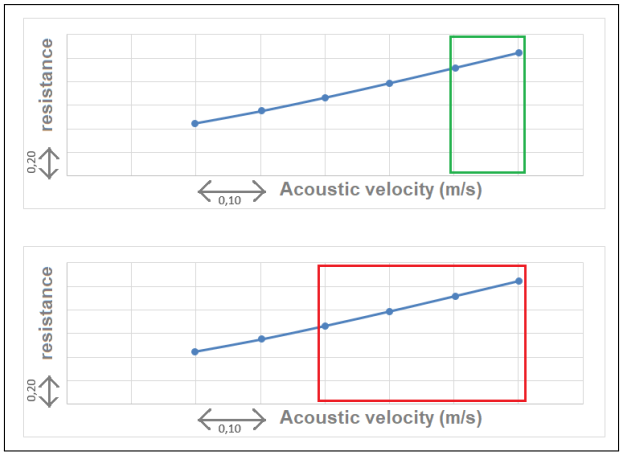

Figure 4. Averaged normalized resistance function of the acoustic velocity of excitation (Conf 3) : linear regression on the intervals [0.6; 0.7] m/s (top) and [0.4; 0.7] m/s (bottom) for the POA computation.

Tab. 1 presents the acoustical POA^{ac} results, which are computed from the NTMM bench measurements with the Eqn. (8), and considering two intervals of acoustic velocity for the linear regression over the resistance, respec-

tively [0.6; 0.7] m/s for the $\text{POA}^{ac}_{0.6\text{-}0.7}$ and [0.4; 0.7] m/s for the $\text{POA}^{ac}_{0.4\text{-}0.7}$. Two samples are measured with the acoustic bench, namely Conf 2 and Conf 3, whereas high resolution pictures are only available on the Conf 3 sample, so that the POA^{ac} results are only available for this sample.

Table 1. Acoustical POA^{ac} results computed from the NTMM bench measurements.

Sample		$\text{POA}^{ac}_{0.6\text{-}0.7}$	$\text{POA}^{ac}_{0.4\text{-}0.7}$
Conf 2	Point 1	4.74	4.69
	Point 2	4.87	4.98
	Point 3	4.92	4.88
	Average	4.84	4.85
	Std Dev	0.093	0.147
Conf 3	Point 1	4.72	4.77
	Point 2	4.93	5.00
	Point 3	4.90	4.94
	Average	4.85	4.90
	Std Dev	0.114	0.119

Tab. 2 presents the optical POA^{op} results, obtained while applying the methodology explained in section 2.3 at the same three 30mm diameter areas of the acoustical measurements of Fig. 1. Once the CHT algorithm has identified the circles and their associated diameter, they are all counted. Some spurious circles are found out of the 30mm diameter of interest, and removed from the final counting. Then, many circles found are blocked, as they are in the upper cavity walls and therefore not opened. Such issue arises because the resistive sheet perforation is done independently of the back cavity, without regard of geometry. This is obviously not the case in an industrial manufacturing process, but could happen for small sampling production as for instance Conf 2 and Conf 3 samples that are made on demand for specific tests. Several examples of these spurious items are presented in the next section 4.

4. ANALYSES AND DISCUSSION

This part presents the outcomes of the first study carried out on the topic by the Airbus acoustic testing team.

Table 2. Optical POA^{op} results of the Conf 3 sample.

Conf 3	POA^{op}
Point 1	5.69
Point 2	5.18
Point 3	6.45
Average	5.77
Std Dev	0.639

Concerning the acoustical POA, the establishment of the non-linear regime in terms of impedance regarding the excitation level is discussed. It is reminded that the linearity of the non-linear evolution is strongly driven by the Reynolds number R_e inside the perforations [15]. It is expressed as a function of the velocity such as Eqn. (9)

$$R_e = \frac{\rho |v| D_h}{\mu} . \tag{9}$$

By observing Fig. 4, the non-linear regime is therefore assumed to be reached, especially for the highest acoustic velocities. In addition, when comparing the results integrated over [0.4; 0.7] and [0.6; 0.7] m/s of Tab. 1, the discrepancies are quite small, which reinforces the previous hypothesis of non-linear regime establishment. Nevertheless, this approach highlights that there is a compromise to make : on the one hand, one can excite and post process many points, which allows to get a more proper mathematical linear regression but is more time consuming, and with a risk of not having fully non-linear regime established; and on the other hand, one idea is to take fewer points only in highest velocities (high Reynolds numbers), and then the linear regression computation could lack of enough points to be relevant. One proposed solution is to get more points in the high velocity regime only, so that it will overcome the problem previously mentioned. The main drawback is that such a regime is dependent on the sample to characterize, and can not be *a priori* estimated, and also that it could be limited by the bench, as the compression driver can not bear very high levels.

By analysing Tab. 1, it can be noticed that the standard deviations computed are quite small, even when considering three positions of the NTMM bench chosen ran-

domly over the sample. This tends to highlight that the sample is relatively homogeneous, and thus the manufacturing satisfying, as well as comfirming the reproducibility of the measurement protocol and bench [1] .

Concerning the POA values obtained by the optical method, Tab. 2 presents a larger standard deviation between the three points. Fig. 5 presents the distribution of the hole diameter (in %) for the Conf 3 sample on average, and for the three areas extracted from the optical computation.

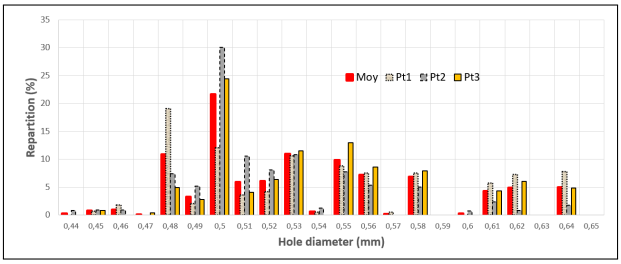

Figure 5. Distribution of the Conf 3 sample hole diameter (%), averaged and for the three areas, from the optical computation.

Several observations can be made from these curves. First, it is reminded that the perforation process consists of several drilling bits mounted on a moving device. Then, the dominant perforation diameter is 0.50 mm, which is the target and therefore is comfirming to assume that both the drilling and the optic methodology are matching the expectations. Third it appears that several diameters are identified by the method, and that some hole diameters are not or barely not represented, such as 0.54, 0.60 or 0.63 mm. It could be assumed that none of these three bits used have these dimensions. Finally, even if there are discrepancies, the curves of the three different locations follow the same tendency, which is once more comforting about the drilling process resulting in homogeneity, as it has been used over all the Conf 3 sample.

Fig. 6 presents many cases of drilled holes obtained on the Conf 3 sample. The image sub-part [A] illustrates regular perforations with several hole diameters identified, whereas the sub-part [B] shows holes that are partially blocked by the walls of the cavity. The latest ones are not fully opened on the volume, but the CHT algorithm identifies them, and with their real drilling diameters, even

[1] This has been validated by previous Airbus internal studies.

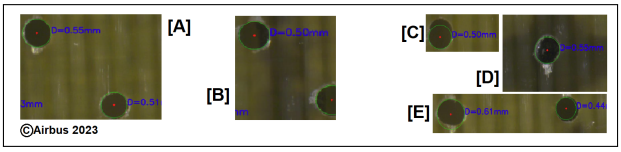

Figure 6. Several close-ups of Conf 3 sample holes : [A] regular holes, [B] partly blocked ones by cavity uprights, [C] double drilling ones, [D] fully blocked one by the cavity walls, and [E] non circular ones.

though they are not completely leading to the cavity behind. The image [C] exhibits a mistake on the drilling process, as the perforation is not cylindrical anymore, but the result of two circles. Such phenomenon could occur for instance when there is a small rebound of the drilling bit on the surface, leading to two perforations very close. The image sub-part [D] presents a hole that is fully blocked by the cavity walls, but is still identified by the CHT algorithm. This case should not exist, as the drilling is completely useless for the acoustic, and unfavorable in terms of drag for a real engine liner. Finally, the picture [E] illustrates non cylindrical holes, which are probably linked to the wear of the drilling bits. Once more, the drilling has not been adapted to the cavity of the studied sample.

The results presented in Tab. 2 take into account : [A] the regular holes; half of the [B] partly blocked ones; the identified diameters of the [C] and [E] holes. This leads to bias in the POA evaluation, that could be either under or over estimated.

It clearly appears that the optical and acoustical POA cannot straightforwardly be compared. Indeed, several aspects have been encountered while performing the present study, and required further analysis on the matter.

First, when considering the acoustical POA, the chosen methodology relies on the liner non-linear regime establishment, with the above mentioned contradictions. To go further, the phenomenon of *vena contracta* [12, 16] could also be more specifically evaluated, with the perforation diameter decrease seen by the acoustic wave, depending on both the velocity and the frequency of excitation. Then, one aspect that is requiring dedicated investigation is the sensitivity of this approach when changing the frequency interval of acoustic resistance averaging. Indeed, the chosen purple area illustrated in Fig. 3 is a plateau of 1 kHz, whereas some authors would rather choose larger plateaus, or the maxima of the resistance,

and therefore not necessarily averaged it on a wide frequency band. Another exploration track could be on the literature side that uses the linear part of the resistance function of the acoustic velocity [17].

Second, when considering the optical POA, it is reminded that the CHT algorithm tested is quite rudimentary, as only fitting perfect circles, and assuming that the perforations are cylindrical. There is therefore a potential bias, because the holes might be slightly conical. Furthermore, this is intrinsically not taking into account forms that are not circles. Additionally, the method sensitivity to the lightning of the first pictures has to be evaluated, as the impact of the picture resolution when compared to the characteristic size of the perforations that have to be identified. This study could also be the opportunity to perform more measurements, as so far only the liner sample presented in this paper has been evaluated. Moreover, some specific attention has to be taken on the identification and sorting between regular holes, and partially or fully blocked holes, which are therefore not contributed to the acoustic efficiency of the liner. Such study could potentially be done thanks to machine learning (with or without pre-tagged training data).

Finally, another POA evaluation techniques might be explored. At the beginning of the study presented in this paper, it had been considered to use a direct geometrical method, by using sub-millimeter pin gauges combined with holes counting in the same areas. However, the laboratory is not equipped with gauges of diameters smaller than 0.52 mm, so that it is not sufficient for the liners of interest (see Fig. 5). One of the main drawbacks would have been that somehow this is a destructive technique because while entering the gauge it could modify the hole shape (conicality for instance) and size (enlarging the perforation). And of course, it is only relevant for perfectly circular holes, and some limitations are also linked to the identification and classification of the partially blocked holes. Another methods could also be envisaged, as multi-axis coordinate measuring machines, or contact-less laser scanners for 2D / 3D profile measurements as used in the manufacturing quality inspection.

5. CONCLUSION

This study presents the experimental percentage of open area (POA) evaluation of an aircraft liner with acoustical and optical methods.

The acoustical approach is based on the direct measurement of the acoustical response of the liner with an impedance tube, which is an in-house bench called NTMM and is presented in this paper. Then, the resistance function of the excitation acoustic velocity is computed, and the resulting acoustical POA is evaluated thanks to a regression of the linear part of the curve, corresponding to the non-linear regime of the liner behaviour, as proposed on the Guess model.

The optical method is based on a high-resolution image of the same liner sample. A Hough transform post-processing is applied to identify the holes and evaluate their diameters, as considered perfectly circular. The optical POA is obtained by counting the areas created by the identified circles over a given area. The study is performed on exactly the three areas of the same sample, materialized by 30 mm diameter holes in an aluminium tape cover.

The acoustical POA exhibits interesting information, as for instance the fact that the sample appears quite homogeneous thanks to a small standard deviation between the different areas. It also permits to strengthen the method reliability, as the results do not depend too much on the acoustic velocity integration of the resistance. However, such behaviour strongly depends on the liner geometry, and no general conclusion could be drawn.

The optical POA results are a first trial of such a method. The chosen liner had been assumed to have only cylindrical perforation, and all holes should have the same diameters. However, one of the main outcomes of this study is that none of these two assumptions are correct. Indeed, it has been observed that several diameters are identified. This is directly linked to the resistive sheet perforation method, where several drilling bits are used simultaneously, leading to a repetitive pattern. In addition, the perforation scheme used is not tailored for the sample, as being a small production for specific tests, whereas in an industrial case, all holes must be fully opening on the backward cavities.

This first study compares two non intrusive and non destructive methods, which have to be further investigated because of exhibiting interesting conclusions and potentials. Indeed, the resistive sheet values usually given by the suppliers are based on the drilling expectations, and not on the effective POA, meaning after the perforation and its bias (non cylindrical holes, wear of the drilling bits, etc.), and also after the liner manufacturing and integration, where the holes can be partially blocked by some migration of the resin into the holes for instance.

In order to continue the development of such a method-

ology, it will be interesting to perform sensitivity studies on several aspects for the two methods. For instance, the frequency interval of resistance averaging has to be investigated for the acoustical POA, as well as a focus on the perforation size for the *vena contracta* phenomenon impact on the non-linear regime. Concerning the optical POA, the picture lightning has to be studied, as the influence of the picture resolution when compared to the characteristic size of the perforations.

6. ACKNOWLEDGMENTS

The first author wants to address his acknowledgments to Olivier Saingès of the Airbus acoustic testing team, for the constant support and time spent on the topic throughout the years.

7. REFERENCES

[1] ICAO, *Annex 16 to the Convention on International Civil Aviation : Environment Protection*, vol. I — Aircraft Noise. International Standards and Recommended Practices, 8^{th} ed., 2020.

[2] Federal Aviation Administration, *Title 14 (Aeronautics and Space), Chapter I (FAA, Department of Transportation), Subchapter C (Aircraft), Part 36 - Noise standards : aircraft type and airworthiness certification, Stage 5*. Code of Federal Regulations, 2017.

[3] U. Ingård and S. Labate, "Acoustic circulation effects and the non-linear impedance of orifices," *The Journal of the Acoustical Society of America*, vol. 22, no. 2, p. 211–218, 1950.

[4] A. Guess, "Calculation of perforated plate liner parameters from specified acoustic resistance and reactance," *Journal of Sound and Vibration*, vol. 40, no. 1, p. 119–137, 1975.

[5] M. Stinson, "The propagation of plane sound waves in narrow and wide circular tubes, and generalization to uniform tubes of arbitrary cross-sectional shape," *The Journal of the Acoustical Society of America*, vol. 89, no. 2, p. 550–558, 1991.

[6] J. Y. Chung and D. A. Blaser, "Transfer function method of measuring in-duct acoustic properties. i. theory," *The Journal of the Acoustical Society of America*, vol. 68, no. 3, p. 907–913, 1980.

[7] J. Y. Chung and D. A. Blaser, "Transfer function method of measuring in-duct acoustic properties. ii. experiment," *The Journal of the Acoustical Society of America*, vol. 68, no. 3, p. 914–921, 1980.

[8] ISO 10534-2:1998, *Acoustics — Determination of sound absorption coefficient and impedance in impedance tubes — Part 2: transfer-function method*. The International Organization for Standardization, 1998.

[9] ASTM E1050-08, *Standard Test Method for Impedance and Absorption of Acoustical Materials Using a Tube, Two Microphones and a Digital Frequency Analysis System*. ASTM International, 2008.

[10] T. Schultz, F. Liu, L. Cattafesta, M. Sheplak, and M. Jones, "A comparison study of normal-incidence acoustic impedance measurements of a perforate liner," 15^{th} *AIAA/CEAS Aeroacoustics Conference (30^{th} AIAA Aeroacoustics Conference)*, vol. 3301, p. 1–14, 2009.

[11] M. Bruneau, *Fundamentals of Acoustics*. Lavoisier, 2006.

[12] U. Ingård and H. Ising, "Acoustic nonlinearity of an orifice," *The Journal of the Acoustical Society of America*, vol. 42, no. 1, p. 6–17, 1967.

[13] I. Sobey, "The occurrence of separation in oscillatory flow," *Journal of Fluid Mechanics*, vol. 134, p. 247–257, 1983.

[14] H. Yuen, J. Princen, J. Illingworth, and J. Kittler, "Comparative study of hough transform methods for circle finding," *Image and Vision Computing*, vol. 8, no. 1, p. 71–77, 1990.

[15] Y. Aurégan and M. Pachebat, "Measurement of the nonlinear behavior of acoustical rigid porous materials," *Physics of Fluids*, vol. 11, no. 6, p. 1342–1345, 1999.

[16] P. Durrieu, G. Hofmans, G. Ajello, R. Boot, Y. Aurégan, A. Hirschberg, and M. C. A. M. Peters, "Quasisteady aero-acoustic response of orifices," *The Journal of the Acoustical Society of America*, vol. 110, no. 4, p. 1859–1872, 2001.

[17] S. Allam and M. Åbom, "Experimental characterization of acoustic liners with extended reaction," 14^{th} *AIAA/CEAS Aeroacoustics Conference (29^{th} AIAA Aeroacoustics Conference)*, vol. 3074, p. 1–14, 2008.